

1 **Combining constraints from tsunami modeling and sedimentology to untangle the**
2 **1969 Ozernoi and 1971 Kamchatskii tsunamis**

3

4 M. Elizabeth Martin¹, Robert Weiss^{2,3}, Joanne Bourgeois¹, Tatiana K. Pinegina⁴, Heidi Houston¹,
5 Vasily V. Titov^{1,2,3}

6

7 ¹Dept. of Earth & Space Sciences, Univ. of Washington, Seattle, WA 98195-1310 USA

8 ²Joint Inst. for the Study of the Atmosphere and Ocean (JISAO), Univ. of Washington, Seattle, WA 98195-4325
9 USA

10 ³Pacific Marine Environmental Laboratory, National Oceanic and Atmospheric Administration, Sand Point Way
11 NE, Seattle, WA 98115 USA

12 ⁴Institute of Volcanology and Seismology, Piip Blvd. 9, Petropavlovsk-Kamchatskiy 683006, Russia

13

14 [1] Large tsunamigenic earthquakes occurred in 1969 (Mw 7.7) and 1971 (Mw 7.8) along the
15 Bering Sea and northernmost Pacific coast of Kamchatka. Both resultant tsunamis were
16 recorded on tide gauges, but only the 1969 tsunami has cataloged observations of runup, and
17 these observations are limited and questionable. We used a combination of field mapping of
18 tsunami deposits and tsunami modeling to augment this historical record. We mapped tsunami
19 deposits above A.D. 1956 and 1964 volcanic ash layers, along more than 200 km of shoreline.
20 However, the 1969 and 1971 tsunami deposits are not distinguishable in the field. The
21 distribution of tsunami-deposit elevation has two latitudinal peaks. From 58° to 57° sediment
22 runup typically ranges from 2 to 4 m, decreasing to the south. From 57° to 56° sediment runup
23 typically ranges from 3 to 6 m [maximum more than 10 m], increasing to the south. Models of
24 local runup for the 1969 and 1971 tsunamis explain most of the sediment distribution,

25 differentiate the two tsunamis in some localities, and elucidate the earthquakes' focal
26 mechanisms and rupture areas.

27

28 **1. Introduction and Background**

29 [2] Even though the Mw 7.7 1969 Ozernoi and the Mw 7.8 1971 Kamchatskii tsunamigenic
30 earthquakes (Fig. 1) occurred in the era of seismic instrumentation, the earthquakes and
31 especially the associated tsunamis are poorly characterized because the region is remote and
32 sparsely populated. Despite shortcomings in historical and instrumental records, however,
33 Kamchatka is an excellent field location for studying tsunami deposits, leading to greater
34 understanding of the earthquakes and their tectonic setting. Foremost, well-studied tephra
35 deposits from prolific volcanoes along the Kamchatka arc provide excellent chronological
36 control. Also, low rates of human, plant and animal disturbance (bioturbation) offer high levels
37 of deposit preservation in peats, beach-ridge swales, and marine terraces. Plate boundaries in the
38 region produce high numbers of earthquakes, and many historical tsunamis have affected
39 Kamchatka (S-Table 1, Fig. 1), leaving geologic traces. In spite of all these favorable conditions,
40 it is still not possible to separate the 1969 and 1971 tsunami deposits through field observations
41 and stratigraphic analysis because dating techniques are not that accurate, and there is not a
42 tephra layer between them (S-Table 1). Previous publications have ascribed all deposits to the
43 1969 tsunami [*Melekestsev and Kurbatov*, 1998; *Bourgeois et al.*, 2006]. In this paper we use
44 sedimentological data coupled with computer modeling of tsunami propagation and inundation
45 in order to examine these two earthquake-generated tsunamis and to answer the following
46 questions. Can we explain all of the deposits with one or the other tsunami, or are both required?

47 Can we explain deposit extent solely by earthquake-induced tsunamis, or must we invoke
48 tsunamigenic landslides?

49

50 **1.1. Tectonic Setting**

51 [3] The northwesternmost Pacific Ocean and southwestern Bering Sea overlie a tectonically
52 complex region; the Mw 7.8 1971 earthquake, though it occurred only a few hundred kilometers
53 from the Mw 7.7 1969 earthquake, was located in a distinctly different tectonic setting (Fig. 1).
54 Moreover, the plate boundaries near these two earthquakes are not well established--geoscientists
55 have subdivided the region into several different plate configurations (six are summarized by
56 *McElfresh et al.* [2002]). In the simplest, 3-plate (Pacific, North America, Eurasia) model,
57 Kamchatka belongs to the North American plate. However, this three-plate model cannot
58 explain the 1969 earthquake [*Pedoja et al.*, 2006], and the 1971 earthquake lies within a complex
59 plate-corner setting, in any model (Fig. 1).

60 [4] In multiplate models, the placement of Kamchatka on the Okhotsk block [*Cooke et al.*,
61 1986; *Apel et al.*, 2006] more easily explains the location and mechanisms of the 1969 and 1971
62 earthquakes. Compression between the Okhotsk block and the Komandorskii Island block
63 occurs in the region of the Kamchatskii Peninsula (Fig. 1), and the inner, southern boundary of
64 the Komandorskii Island block is the locality of the 1971 earthquake. To the north, compression
65 occurs between a rotating Bering block [*Mackey et al.*, 1997] and the Okhotsk block, and this
66 boundary is the site of the 1969 Ozernoi earthquake. The April 2006 Koryak (or Olyutorskii)
67 earthquake (Fig. 1) also occurred on the (proposed) Bering/North America boundary [*Rogozhin*
68 *et al.*, 2006].

69

70 **1.2. The 1969 Ozernoi earthquake and tsunami**

71 [5] On 22 November 1969 at 23:09 local time, a Mw 7.7 [*Gusev and Shumilina*, 2004] thrust
72 earthquake occurred off the Ozernoi Peninsula, Russia, in the western Bering Sea (Fig. 1).
73 Originally, *Fedotov and Gusev* [1973] concluded that the fault plane was nearly vertical and the
74 earthquake was strike-slip. Later, *Cormier* [1975] and *Daughton* [1990] concluded the 1969
75 earthquake was a low-angle (5-10°) thrust. The associated tsunami, though it had little human
76 impact due to sparse population, was described at a number of local sites, with a maximum
77 reported runup of 10-15 m on the Ozernoi Peninsula (S-Table 1). Several workers have
78 suggested that a landslide associated with the 1969 earthquake caused this reported high runup
79 [*Zayakin*, 1981; *Melekestsev*, 1995; *Gusiakov*, 2003]. The tsunami was also recorded on local
80 tide gauges in Ust' Kamchatsk and Petropavlovsk-Kamchatskii, as well as far-field sites
81 including Hilo (S-Table 1).

82 [6] Deposits from the 1969 tsunami were reported by *Melekestsev and Kurbatov* [1998] from
83 Karaginsky Island (Fig. 1c), along with evidence that the tsunami had changed the course of a
84 stream, an oxbow cutoff. *Bourgeois et al.* [2006] described tsunami deposits attributed to 1969
85 in southern Ozernoi Bay. Based on tsunami deposit distribution, Titov in a preliminary model of
86 the tsunami used a low-angle thrust with 3.5 m horizontal shortening during the 1969 earthquake
87 [*Bourgeois et al.*, 2004].

88

89 **1.3. The 1971 Kamchatskii earthquake and tsunami**

90 [7] On 15 December 1971 at 20:30 local time a Mw 7.8 [*Gusev and Shumilina*, 2004]
91 oblique-thrust earthquake occurred off the Kamchatskii Peninsula near the line of demarcation
92 between the Bering Sea and Pacific Ocean (Fig. 1). *Gusev* [1975] documented observations of

93 the 1971 earthquake and tsunami including building destruction in Ust' Kamchatsk and on the
94 Kamchatskii Peninsula, tide-gauge records of the tsunami, and reports of ice cracking 1 km up
95 the Kamchatka River from Ust' Kamchatsk, probably from the tsunami. *Cormier* [1975] and
96 *Okal and Talandier* [1986] resolved thrust mechanisms for the earthquake.

97 [8] There are no recorded eyewitness accounts of the tsunami or prior publication about
98 tsunami deposits from the 1971 tsunami. Tide-gauge records from Ust' Kamchatsk and Hilo (S-
99 Table 1) indicate that in these locations 1971 tsunami amplitude was about twice that of the 1969
100 tsunami, as expected, given size of the earthquake and location of the tsunami source area.

101

102 **2. Tsunami deposits**

103 **2.1. Field methods**

104 [9] Field work was carried out in the summers of 1999, 2000, and 2002-2004 in seven
105 locations along the Bering Sea coast of Kamchatka from north of the Uka River to the
106 Kamchatskii Peninsula and Bering Island (Fig. 2). The coastline in this region varies from long
107 series of low beach ridges (e.g., Uka) to steeply sloping coasts and narrow beach plains (e.g.,
108 Kamchatskii Cape) (Figs. S1-S3). Field methods were as in *Bourgeois et al.* [2006], including
109 topographic profiling with a transit and rod, and multiple trench-like excavations along profiles
110 (see S6). All profiles were measured beyond the extent of the deposit. To provide consistency
111 among profiles, we normalized the height and distance inland of the deposits with respect to the
112 high tide mark because we assume that this datum does not change considerably along the
113 explored sections of coastline. The 1969 tsunami occurred near high tide, but the 1971 tsunami
114 occurred near low tide; tide range in the region is $\sim 1.5 \pm 0.5$ m.

115 **2.2 Field results**

116 [10] In all seven field locations, in 59 of 77 profiles (Figs. S1-S3), we found a tsunami deposit
117 [or possible tsunami deposit] above either the 1956 or 1964 tephra (Figure 1C). In 57 cases, the
118 last excavation clearly did not contain the deposit. This deposit, comprising sand and fine gravel
119 transported from the beach, is typically a few centimeters thick, ranging up to 20 cm. We call
120 the elevation of the deposit at its maximum horizontal extent inland “sediment runup.”

121 [Maximum extent inland is defined as *inundation*.] The distribution of tsunami-deposit elevation
122 has two latitudinal peaks (Fig. 2). From 58° to 57° sediment runup typically ranges from 2 to 4
123 m, decreasing to the south. From 57° to 56° sediment runup typically ranges from 3 to 6 m
124 [maximum more than 10 m], increasing to the south.

125 [11] On the Ozernoi Peninsula, we measured maximum sediment runup of about 4 m above
126 high tide, significantly lower than reported catalog runup observations of 10-15 m south of Cape
127 Ozernoi [Zayakin, 1981]. This and other discrepancies could be due in part to sediment extent
128 being less than actual tsunami wave runup/inundation. However, we think maximum deposit
129 elevations on the Ozernoi Peninsula, as well as modeling described below, cast doubt on the 10-
130 15-m cataloged runup.

131 [12] In general, sediment extent is greatest on Ozernoi and Kamchatskii peninsulas, which are
132 also the areas with some of the steepest profiles (Figs. S1-S3). In areas such as Ozernaya and
133 Uka (Fig. 2), profile elevations rarely exceed 5 m above high tide (Table S5), so though the
134 tsunami may have been higher than 5 m, there will be no sedimentological evidence left behind.
135 On these low profiles, however, the deposit can extend farther inland.

136

137 **3. Tsunami Modeling**

138 **3.1. Methods**

139 [13] Tsunami modeling is done in two stages. The first stage is the computation of initial
140 deformation of the ocean surface due to the earthquake, which is used as initial conditions for a
141 tsunami propagation model. The second stage is computation of tsunami wave evolution
142 including runup. For each earthquake, after preliminary runs, we tested five initial conditions
143 based on the given parameter range from seismologic analysis (Table 1). We used the MOST
144 (Method of Splitting Tsunami, *Titov and Synolakis* [1995, 1998]) model to generate runup. Our
145 goal was to vary initial conditions to find the best match of modeled tsunami runup with the
146 minimum runup indicated by tsunami deposits.

147 [14] To determine the source mechanisms that best explain our field sedimentological
148 observations we started with published focal mechanisms [*Cormier, 1975; Okal and Talandier*
149 *1986; Daughton, 1990*] (Fig. 1; Table 1). We held the seismic moment constant for each
150 earthquake and used the same shear modulus [30 GP] in all cases. Because the published focal
151 mechanisms do not completely agree, and because each focal mechanism represents two possible
152 fault planes, we started with four possible fault-plane solutions for each earthquake (each had
153 two published focal mechanisms). We ran preliminary models were run for all four
154 configurations, but favored the low-angle solution for both 1969 and 1971 based on published
155 data, local structures, and tectonic setting. Then, using mapped aftershocks of each earthquake,
156 we varied rupture location, slip, length and width. We then used equations derived by *Okada*
157 [1985] to compute surface deformation--the initial tsunami condition.

158 [15] To model tsunami wave evolution including runup, we used the MOST code with
159 three telescoping grids. In the first two grids (resolutions 90 and 27 arcsec) the shallow-water
160 wave equations (SWE) are numerically solved with reflective boundaries for land, and radiating
161 boundaries for water to account for propagation. The third grid has a resolution of 3 arcsec, and

162 in this case the SWE are solved with radiating boundaries for water, and a moving boundary for
163 land to account for inundation. Finally, in order to constrain model parameters, for each
164 simulated tsunami we made comparisons of time series of the model output to tide-gauge records
165 from Ust' Kamchatsk (Fig. S4). Given uncertainties in bathymetry, tide-gauge location, and
166 quality of tide-gauge records, these comparisons are difficult; but remain an important means to
167 gain confidence in the tsunami sources we used.

168

169 **3.2. Modeling Results**

170 [16] Modeling of the two tsunamis indicates that most of the identified deposits can be
171 explained by the 1969 and 1971 earthquakes (Fig. 2). Inundation computations using MOST
172 showed that both earthquakes generated significant tsunamis in the region of field investigations
173 (Fig. 2, 3), and both tsunamis are needed to explain the field data. Model runup of the 1969
174 tsunami is highest on the Ozernoi Peninsula and also north of the Stolbovaya field area (Fig.
175 2,3); the latter is a region where we have no field data because the coastline is dominated by
176 cliffs. Model runup of the 1971 tsunami is highest on the Kamchatskii Peninsula (Fig. 2,3).

177 [17] In general, deposits from field areas to the north—Uka, Ozernoi, and Ozernaya—are in
178 good agreement with the preferred model of the 1969 tsunami, and deposits to the south—
179 Soldatskaya and Kamchatskii—are in good agreement with the 1971 model (Fig. 2). The source
180 of the deposits in Stolbovaya is ambiguous (Fig. 2). Catalog data of runup for 1969 (S-Table 1;
181 Fig. 2) are slightly higher than computed runup values in most localities, and much higher just
182 south of Cape Ozernoi. The field data agree better with model results than with catalog data, so
183 we are inclined to interpret the catalog data as exaggerated.

184

185 **4. Discussion and conclusions**

186 [18] We conclude that modeled initial conditions can explain most of the tsunami-deposit
187 distribution (Fig. 2, 3) without invoking submarine landslides. However, lack of available high-
188 resolution topographic and bathymetric data did not allow us to compare model results with
189 sedimentological data on a profile-by-profile scale. Also, because modeling with MOST is
190 limited to water dynamics and does not involve sediment transport directly, model results must
191 be achieved that show runup values higher than sediment data. In comparison, reported
192 observations of tsunami runup from the catalog would be expected to be similar to modeled
193 heights, though eyewitnesses commonly overestimate tsunami runup. If a landslide augmented
194 tsunami runup, sediment and catalog heights would be expected to be higher than modeled
195 heights, possibly only in one field area.

196 [19] Only one site—Stolbovaya (56.6-56.8° N)—shows significant discrepancies between
197 the model and sediment data (Fig. 2). These discrepancies may be explained by limitations in the
198 model, particularly of bathymetric resolution, or by a local submarine landslide from the nearby
199 submarine canyon, or both. Local submarine landslides, which commonly are earthquake-
200 triggered, are possible throughout region due to steep bathymetric gradients and to river-supplied
201 sediments. However, given uncertainties in determining initial conditions from seismologic
202 analyses, and limitations in available bathymetric data, there is no clear need to invoke
203 submarine landslides. Further, and in any case, a local submarine landslide off northern
204 Kamchatka would generate highly dispersive waves)[e.g., *Lynette and Liu, 2003*] which would
205 not produce a recognizable signature on far-field tide gages such as Hilo, 5000 km away (S-
206 Table 1)

207 [20] Tsunami modeling indicates that, although there are no catalog data for 1971 tsunami
208 runup, sand deposits on the Kamchatskii Peninsula were most likely deposited by the 1971
209 tsunami, rather than the 1969 tsunami. Thus this study extends our knowledge of the largely
210 ignored 1971 tsunami, for which there are few cataloged or recorded observations. In a region of
211 complex tectonics, the 1971 earthquake shows the potential for large oblique-thrust earthquakes
212 in an area close to, but not on, a major active plate boundary and may be an indicator of more
213 diffuse stresses in the Kamchatskii Peninsula region.

214

215 **Acknowledgments**

216 This project was supported principally by NSF EAR 0125787 to Bourgeois, RFBR 00-05-64697
217 and 03-05-64584 to Pinegina. We thank V. Ponomareva, E. Kravchunovskaya, K. Pedoja, V.
218 Alvarez, V. Morose and many other field participants.

219

220 **References**

- 221 Apel, E. V., R. Bürgmann, G. Steblov, N. Vasilenko, R. King, and A. Prytkov. (2006),
222 Independent active microplate tectonics of northeast Asia from GPS velocities and block
223 modeling. *Geophysical Research Letters*, 33, L11303, doi:10.1029/2006GL026077
- 224 Bourgeois, J., V. Titov, and T. Pinegina (2004), Subduction-zone behavior backed out of tsunami
225 deposits, Kamchatka, far eastern Russia. *Proceedings Japan-Kuril-Aleutian Workshop on*
226 *Subduction Processes (JKASP)*, 97-98.
- 227 Bourgeois, J., T. Pinegina, V. Ponomareva, and N. Zaretskaia (2006), Holocene tsunamis in the
228 southwestern Bering Sea, Russia Far East, and their tectonic implications. *Bulletin of the*
229 *Geological Society of America*, 118(3/4), 449-463.

230 Cook, D. B., K. Fujita, and C. McMullen. (1986), Present-day plate interactions in northeast
231 Asia: North American, Eurasian, and Okhotsk plate, *Journal of Geodynamics*, 6, 33-51.

232 Cormier, V. F. (1975) Tectonics near the junction of the Aleutian and Kuril-Kamchatka arcs and
233 a mechanism for middle Tertiary magmatism in the Kamchatka basin, *Bulletin of the*
234 *Geological Society of America*, 86, 443-453.

235 Daughton, T. M. (1990), Focal mechanism of the 22 November 1969 Kamchatka earthquake
236 from teleseismic waveform analysis, *Keck Research Symposium in Geology*, 3, 128-131.

237 Fedotov, S. A., and A. Gusev (1973), Ozernoi earthquake and tsunami 22 (23) November 1969,
238 *Earthquakes in the USSR in 1969: Nauka*: 195-208.

239 Gusev, A.A. (1975), Earthquakes in the USSR from the year 1971. USSR Academy of Science,
240 Science Publishing House, Moscow, Russia, 172-183 (in Russian).

241 Gusev, A. A., and L. Shumilina (2004), Recurrence of Kamchatka earthquakes on a scale of
242 moment magnitude, *Izvestiya-Physics of the Solid Earth*, 40(4), 206-215.

243 Gusiakov, V.K. (2003), Identification of slide-generated tsunamis in the historical catalogues, in
244 Submarine Landslides and Tsunamis, Yalciner, A.C., Pelinovsky, E.N., Okal, E., and
245 Synolakis, C.E., eds., *NATO Earth and Environmental Sciences* 21, 25-32.

246 Lynett, P., and P. L.-F. Liu (2004), Submarine landslide generated waves modeled using depth-
247 integrated equations, in Submarine Landslides and Tsunamis, Yalciner, A.C., et al., eds.,
248 *NATO Earth and Environmental Sciences* 21, 51-58.

249 Mackey, K. G., K. Fujita, L. Gunbina, V. Kovalev, V. Imaev, and B. Kozmin. (1997), Seismicity
250 of the Bering Strait region: evidence for a Bering block, *Geology*, 25, 979-982.

251 McElfresh, S. B. Z., W. Harbert, C. Ku, and J. Lin. (2002), Stress modeling of tectonic blocks at
252 Cape Kamchatka, Russia using principal stress proxies from high-resolution SAR: new
253 evidence for the Komandorskiy Block, *Tectonophysics*, 354, 239-256.

254 Melekestsev, I. V., 1995. On the possible source of the November 23, 1969 Ozernoi tsunami in
255 Kamchatka, *Volcanology and Seismology*, 17, 361-364.

256 Melekestsev, I. V., and A. Kurbatov. (1998), Frequency of large paleoearthquakes at the
257 northwestern coast of the Bering Sea and in the Kamchatka basin during late
258 Pleistocene/Holocene time, *Volcanology and Seismology*, 19, 257-267.

259 Okada, R. (1985), Surface deformation due to shear and tensile faults in a half-space, *Bulletin of*
260 *the Seismological Society of America*, 75(4), 1135-1154.

261 Okal, E. A., and J. Talandier. (1986), T-wave duration, magnitudes and seismic moment of an
262 earthquake-application to tsunami warning, *Journal of Physics of the Earth*, 34, 19-42.

263 Pedoja, K., J. Bourgeois, T. Pinegina, and B. Higman (2006), Does Kamchatka belong to North
264 America? An extruding Okhotsk block suggested by coastal neotectonics of the Ozernoi
265 Peninsula, Kamchatka, Russia, *Geology*, 34(5), 353-356.

266 Rogozhin, E.A., E.E. Gordeev and V.N. Chebrov (2007), The Koryak strong earthquake of
267 April 20 (21), 2006: Preliminary results, *Izvestiya Physics of the Solid Earth*, 43(2), 103-110,
268 1069-3513, 10.1134/S1069351307020012.

269 Titov, V. V., and C. Synolakis. (1995), Modeling of breaking and nonbreaking long-wave
270 evolution and runup using VTCS-2, *Journal of Waterways, Ports and Ocean Engineers*, 121,
271 308-316.

272 Titov, V. V., and C. Synolakis. (1998), Numerical modeling of tidal wave runup, *Journal of*
273 *Waterway, Port, Coastal and Ocean Engineering*, 124(4), 157-171.

- 274 Zayakin, Y. A. (1981), The tsunami of 23 November 1969 at Kamchatka and certain aspects of
275 its occurrence, *Meteorologiya i Gidrologiya*, 12, 77-83.
- 276 Zayakin, Y. A., and A. Luchinina. (1987), *Catalogue of Tsunamis on Kamchatka*: Obninsk, 50p.
277

277
278 Figure 1. A. Location of the field area and tectonic setting, with Pacific plate motion relative to
279 North America. B. Approximate source area of selected historical tsunamis C. Tephra and
280 earthquake locations referred to in this study, including one-week aftershocks of the 1969 and
281 1971 earthquakes; additional proposed plate boundaries shown in dashed lines (see text for
282 references).

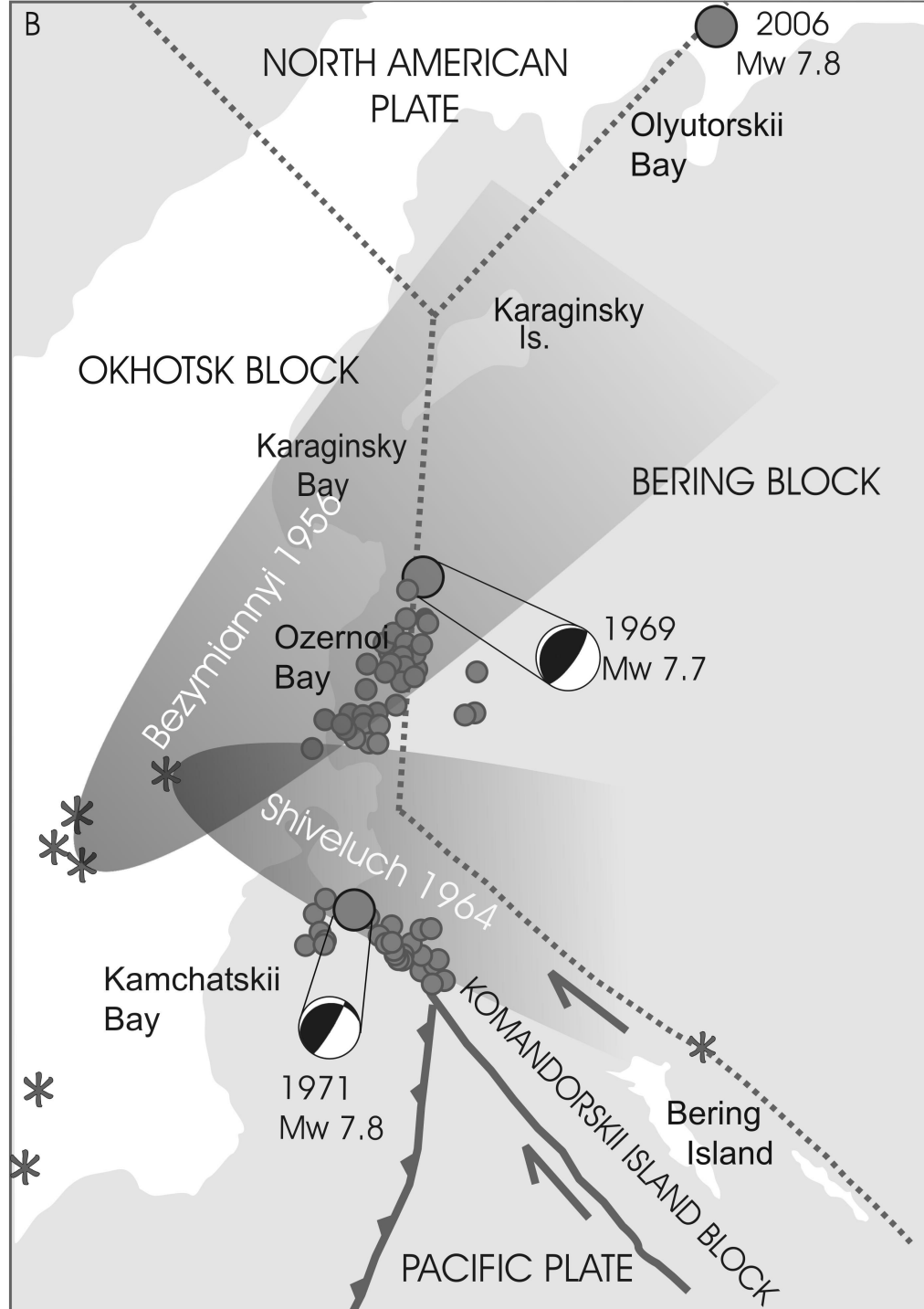
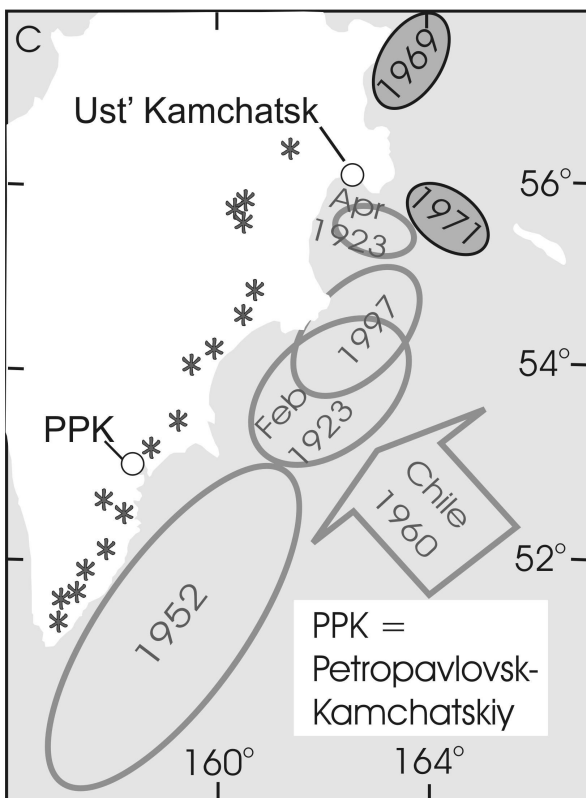
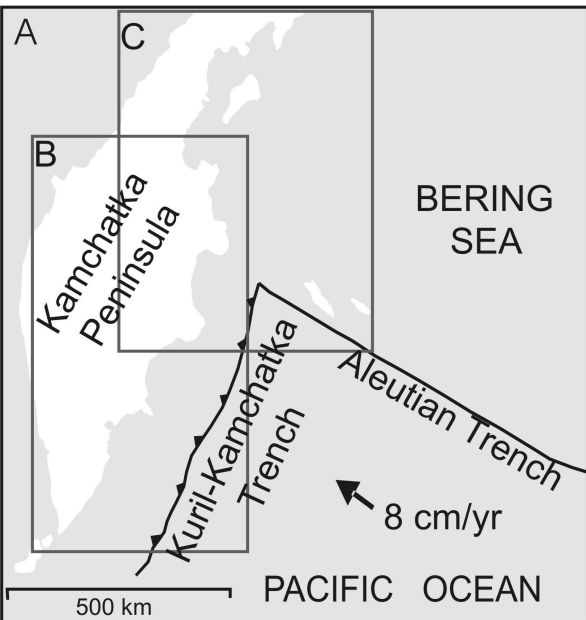
283
284 Figure 2. A: Elevation distribution of tsunami deposits discussed in the text (see also
285 Figs. S1-S3. “Height at maximum distance inland” is what is usually termed runup, and
286 modeling gives a comparable value, at the limit of inundation. Maximum height of the deposit,
287 where that number is greater than runup, is also given. B: Comparison of field sediment heights
288 to runup modeled for the 1969 and 1971 tsunamis, plotted by latitude. Dot-dash line shows
289 envelope of field sediment runup, excepting outliers. Shaded areas, shown for visual ease, are
290 very simplified because runup models were run only where we had topographic profiles; see
291 figure 3 for the overall pattern of tsunami amplitude. Modeled runup should exceed sediment
292 runup (field data) to satisfy conditions for a fit. The 1969 model exceeds field data in the north,
293 the 1971 model exceeds field data in the south, and neither exceeds the data in the middle.

294
295 Figure 3: Maximum plot of wave elevation from preferred model runs. A) 1969h B) 1971c
296 (parameters given in Table 1).

Table 1. Parameters used for initial deformation for MOST model runs (preferred runs in bold)

Run	Longitude [°E]	Latitude [°N]	Length [km]	Width [km]	Dip [°]	Rake [°]	Strike [°]	Slip [m]	Depth [km]
1969d	163.1	57.4	100	50	14	90	210	3.5	5
1969e	163.1	57.6	100	50	14	90	210	3.5	5
1969f	163.1	57.4	71	71	14	90	210	3.5	5
1969g	163.1	57.4	100	50	14	90	210	4.5	5
1969h	163.1	57.3	100	50	14	90	210	3.5	5
1971c	164	55.8	100	50	12	53	258	8	5
1971d	164	55.8	71	71	12	53	258	8	5
1971e	163.9	55.8	100	50	12	53	258	8	5
1971f	164	55.9	100	50	12	53	258	8	5
1971g	163.26	56	100	50	11	55	330	8	5

Notes: original sources for model parameters: 1969d -- Daughton (1990), Cormier (1975);
1971c – Okal and Talandier (1986); 1971g -- Cormier (1975)



○ Approximate tsunami source

○ Location of tide gauge

— Aleutian trench

● Tephra

* Historically active volcano

● Earthquake epicenter

— Subduction zone

..... Possible plate boundary

